

numbering identification scheme is overlain on the image. Figure 7.10 includes *Mariner 10* photomosaics of the north and south polar regions showing some of the larger craters with radar bright deposits.

The current evidence suggests that Mercury's polar deposits are probably water ice. The most likely sources of the water are micrometeorite, comet, and water-rich asteroid impacts. Extrapolating the current terrestrial influx of interplanetary dust particles to that at Mercury indicates that continual micrometeorite bombardment of Mercury over the last 3.5 billion years could have delivered  $3\text{--}60 \times 10^{15}$  kg of water ice to the permanently shadowed polar regions (an average thickness of 0.8–20 m). Impacts from Jupiter-family comets over the last 3.5 billion years can supply  $0.1\text{--}200 \times 10^{13}$  kg of water to Mercury's polar regions (corresponding to an ice layer between 0.05–60 m thick). Halley-type comets can supply  $0.2\text{--}20 \times 10^{16}$  g of water to the poles (0.1–8 m ice thickness). These sources provide more than enough water to account for the estimated volume of ice at the poles. The ice deposits could, at least in part, be relatively recent deposits, if the two radar features A and B were the result of recent cometary or water-rich asteroid impacts.

While the evidence for water ice is strong, other possibilities for the material causing the high radar backscatter signal have been suggested. Unfortunately, until this discovery there has not been much need for ground-based laboratory experiments to determine the radar properties of planetary materials. During and following World War II, there were some measurements of a variety of materials of interest to the military. Among them was sulfur ( $S_0, n = 2, 4, \dots$ ), a substance used as an electrical insulator. One property of a good radar backscattering material is that it is a good electrical insulator, sulfur is such a substance. A source of sulfur is the constant rain of meteoritic material. The problem with sulfur being the deposits on Mercury is that it is stable at higher temperatures than water, and there are no highly radar backscatter deposits in the polar regions where temperatures are within the stability range of sulfur. A 1-meter thick layer of water ice is stable for one billion years at a temperature of  $-161^\circ\text{C}$  while sulfur is stable at a considerably higher temperature of  $-55^\circ\text{C}$ . Much of the region surrounding permanently shadowed craters is less than  $-55^\circ\text{C}$ , but there are no radar reflective deposits there. Very cold silicate glass has also been suggested as a possibility. The *MESSENGER* mission to Mercury should be able to address this problem from critical measurements made during its orbital lifetime.

## 8

### Surface composition

#### 8.1 ALBEDO AND COLOR

*Mariner 10* made no measurements that could determine the elemental abundances, specific minerals, or rock types on Mercury. All we know about Mercury's surface composition comes from ground-based observations and inferences from color reconstructions of *Mariner 10* images. Recalibrations of the *Mariner 10* images and a technique of ratioing images and looking at relative brightness from two different colors has resulted in several important new insights into the makeup of the *regolith* and possibly its iron oxide (FeO) content. They have also suggested the location of compositional boundaries.

*Albedo* is one word used to quantify the percentage of light reflected back from a surface. The albedo of Mercury's surface varies from one location to another and from one wavelength to another. The human eye is sensitive to the spectral range from about 400 to 700 nm and perceives what we call the *visible spectrum*. The colors violet, indigo, blue, green, yellow, orange, and red all fall within that range. Other wavelength ranges are also referred to as having colors, just not visible colors. One way planetary surfaces are compared in their scattering and compositional characteristics is by their color. Often the color may refer to the relative albedo at one spectral region to the albedo of a different planetary surface (or atmosphere) at the same wavelength interval. The albedo of a surface will also vary when the angle of incidence and exitance of reflecting sunlight changes. Thus, to properly compare different albedo measurements, not only must the location be known but also the illumination geometry must be the same on both surfaces being compared. Thus, researchers must be careful to make comparisons that are justified within the experimental uncertainties.

### 8.1.1 Mercury's EUV, UV-VIS, and near-IR albedo

Observations of the day side albedos of the Moon and Mercury were made by *Martiner 10* with the airglow spectrometer (extreme ultraviolet-[EUV]) and the imaging experiment (3300 Å to ultraviolet [UV]). Analysis of these data showed Mercury's surface to have lower overall EUV albedo than the Moon by a few percent. In addition, Mercury's EUV albedo is somewhat higher at the shorter wavelengths (600–1000 Å) than at longer wavelengths (1000–1650 Å). However, the albedo rapidly rises in the UV from 1600–4000 Å. It continues to rise through the visible and the near-infrared (IR) to 10,000 Å. Different regions on the surface have different albedos at the same wavelength. For example, fresh craters and crater rays are very bright, having higher albedos than the darker surrounding regions.

The composition of the surface materials plays an important role in explaining the albedo of the surface. So does the grain size and porosity of the surface materials. For example, finely crystalline silicates low in iron and titanium tend to be brighter and scatter more light off the surface.

*Martiner 10* obtained many images of the surface with the visible light filter (V) that is centered on 554 nm. There were enough images obtained to permit comparison of albedos from many locations. These measurements were compared to albedo measurements of the Moon made at 5° phase angle by using modeling techniques. Table 8.1 compares the albedo from regions on Mercury's surface to similar landforms on the Moon.

From Table 8.1, it appears that Mercury has a higher albedo in the visible (VIS) wavelength range than the Moon at some locations. This may indicate important compositional differences between Mercury and the Moon. In addition, Mercury albedos tend to be more uniform in the UV-VIS than those of the Moon which vary greatly from maria to highlands. Exceptions to the uniform albedos are the brightest rays on Mercury which show the highest albedos in Table 8.1.

**Table 8.1.** Comparison of albedo from regions on Mercury's surface to similar landforms on the Moon.

Terrain	Albedo at 554 nm wavelength (visible) normalized to 5° phase angle
Mercury Caloris smooth plains	0.12–0.13
Lunar maria	0.06–0.07
Mercury highlands (intercrater plains)	0.16–0.18
Lunar highlands	0.10–0.11
Mercury bright rayed craters	0.36–0.41
Lunar bright rayed craters	0.15–0.16

### 8.1.2 Changes of albedo with phase change

It has been known for centuries that as the Moon changes in phase from a thin crescent to full, the brightness of the surface increases dramatically. This increase in brightness is much more than could be accounted for by just having more of the surface illuminated by the Sun as the *phase angle* decreased (the Moon approached full phase). The extra light coming from the surface is, in part, a consequence of a decrease in the amount of shadowing of reflected light from the surface as the light path becomes more and more direct (perpendicular to the surface) from the Sun. A decade ago, Bruce Hapke, a planetary scientist at the University of Pittsburgh, showed that the increase in light near full phase is also because the light entering the soil particles scattered out toward the observer with the same electromagnetic wave properties as it entered. This phenomenon, called coherence, increases the amplitude of the light and contributes to the surge of light near full phase. The overall shape of the phase curve is diagnostic of backscattering efficiency, particle size, microscopic roughness, and other properties of the surface materials.

During the past few years, Mercury was observed by instrumentation on the *Solar Heliospheric Observer (SOHO)* from Earth orbit, obtaining several new data points near 180° phase angle (thin crescent). These added points have enabled scientists to study the entire phase behavior of both the Moon and Mercury. Mercury exhibits slightly more backscattering than the Moon near full phase (has a sharper peak near 0° phase angle). This can be seen in Figure 8.1. The curves in the figure are based on models of the scattering behavior of the powdered surface of an airless planet. Such models make predictions on the physical and optical structure of the small grains in the topmost 1 mm of the surface, which is the region where sunlight is scattered, reflected, and absorbed by the particles before eventually reaching the telescope. From such modeling, we have reason to believe that there are other differences as well between the regolith of the Moon and Mercury. For example, it seems that Mercury's surface grains are smaller and more transparent than their lunar counterparts. They also seem to reflect light more effectively towards the direction of the Sun, which may be due to the presence of complex or fractured grains. Particles with these properties are known from the Moon as glassy conglomerates of rocky grains called *agglutinates*, formed during heat generating impacts. The inference is that such particles are more common on Mercury, are less dark, or are more complex. The high *transparency* goes hand in hand with results from other studies that indicate that the surface is generally much poorer in iron and its compounds, darkening constituents, than the Moon's surface. In addition, Mercury's surface seems to be smoother than the Moon's.

### 8.1.3 Spectral slope and "maturity"

Reflected light from silicate regoliths of airless bodies like Mercury and the Moon have been studied for decades with the hope of isolating specific physical properties

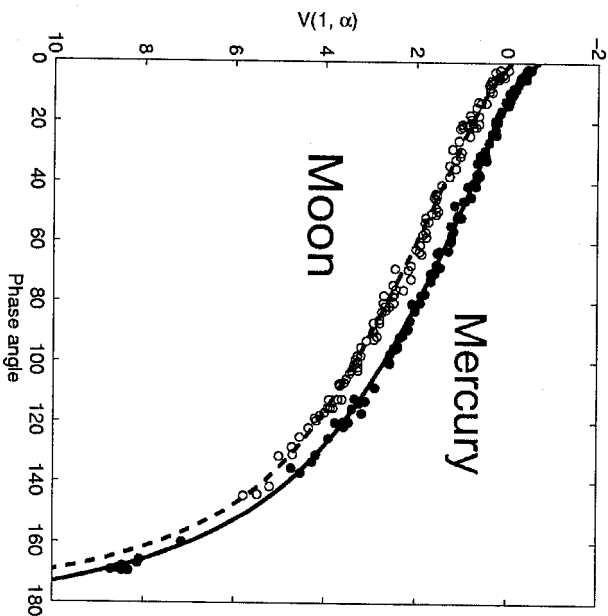


Figure 8.1. Phase curves for Mercury and the Moon. The total light coming from the planet as it changes phase from crescent to full is measured and plotted. The brightness of Mercury (top) and the Moon (bottom) in the V filter band (visible wavelengths) is scaled to the same distance (1 AU) to the Sun and the Earth. Though the two best-fit curves drawn through the observed data points are similar they are not exactly the same, which indicates different light scattering behavior for the two bodies. There is uncertainty in the absolute brightness when the two curves are adjusted for the actual size of the Earth-facing disk. Such an adjustment has not been made for the curves shown here (courtesy of Johan Warrell, University of Uppsala, Sweden).

that can be inferred from spectral features and from *spectral slope*. The task has not been an easy one because there are many variables such as composition and grain size that vary among the terrestrial planets. In addition, the amount of glassy material formed by impact, the effects of impacting ions and electrons on color and crystalline lattice structure, the degree to which the surface is protected from charged particles by magnetic fields, and the age of the regolith also confound an easy answer. But, because of the tenacity of researchers seeking to understand distant regoliths in the Solar System, much progress has been made. Today most researchers would agree that spectral slope is an indicator of the degree to which the surface has been altered by external processes such as the

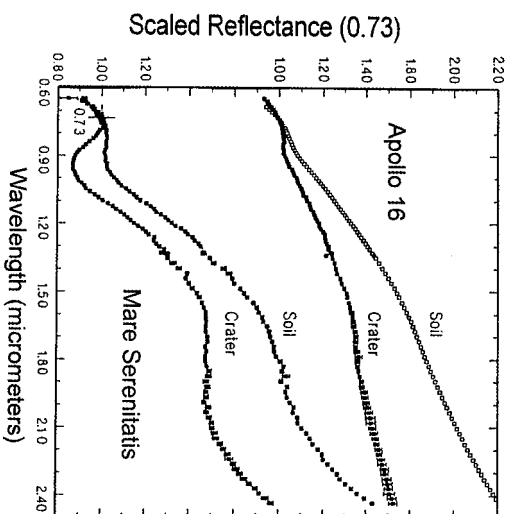


Figure 8.2. Regions on the Moon that have similar composition have different spectral slopes because of different amounts of space weathering. The slope is steeper from shorter to longer wavelength (left to right) as the surface becomes more mature (adapted from Pieters and Engler, 1993).

ones listed above. Such alterations are called space weathering (for details refer to the discussion at the end of Chapter 5.) Freshly exposed rock and soil from a recent impact has not experienced much space weathering, while ancient terrains are highly altered by space weathering. We call the degree to which the surface has been altered, the maturity of the surface. A soil, freshly exposed by an impact is an *immature* soil. A soil that has been exposed to the effects of space weathering for two billion years is said to be *mature*.

*Spectral slope* is a major indicator of soil maturity. Most of our knowledge regarding this relationship between slope and maturity comes from studying the Moon and to a lesser degree, the asteroids. The spectral slope of many different lithologies on the Moon is well known. Spectra of small areas on the Moon with similar compositions have different slopes because of different maturities. This is illustrated in Figure 8.2 where lunar soils in and near to craters are compared to soils undisturbed by the impact.

Mercury's *reflectance* between 400 and 1000 nm has been very well measured in the last decade because such measurements can be made from ground-based telescopes with modest size mirrors and grating spectrographs. Recent photometric observations of the Earth-facing hemisphere of Mercury not imaged by Mariner 10 were obtained in 1997 and 1998 with the Swedish Vacuum Solar Telescope on

La Palma in the Canary Islands. The spectrum of Mercury was found to have a linear slope from 650 to 940 nm, indicating that the average Mercurian regolith is considerably more mature than "near-side" lunar immature anorthositic regolith. These observations also found that Mercury's surface is more backscattering than that of the Moon at these wavelengths. This wavelength range is discussed in more detail in the sections below.

## 8.2 MATERIALS OF TERRESTRIAL PLANETARY SURFACES

The most common solid materials on Earth are rocks and soils that are made up mostly of oxygen (O) and silicon (Si). Many minerals are *solid solutions*, in varying proportions, of the oxides of silicon (Si), calcium (Ca), aluminum (Al), magnesium (Mg), sodium (Na) and potassium (K). Rocks formed from such minerals are called *silicates*. Minerals form with specific combinations of these elements based upon atomic radius, distribution of electrons, and other important characteristics of chemical bonding. Iron plays an especially interesting role in that it can be present as a component of silicates (oxides) or it can be present as a separate metallic phase along with nickel, sulfur and certain other elements. Common rock-forming minerals include feldspar, pyroxene, olivine, and iron-titanium oxides.

On Earth, feldspars are the most abundant of all minerals in the crust. While closely related, they fall into groups: potassium and barium (Ba) feldspars, or sodium and calcium feldspars for example. The types have different crystalline structures. The structure of feldspars is a continuous three-dimensional network of SiO<sub>4</sub> and AlO<sub>4</sub> tetrahedra. The structure is elastic and adjusts itself to the size of cations that occupy the interstitial openings of the chain. If the cations are large (K, Ba), the feldspar formed may be orthoclase (KAlSi<sub>3</sub>O<sub>8</sub>). If the cations in the interstitial openings are small (Ca, Na), the feldspar may be albite (NaAlSi<sub>3</sub>O<sub>8</sub>), or Ca-rich anorthite (CaAl<sub>2</sub>Si<sub>2</sub>O<sub>8</sub>). Orthoclase, albite, and anorthite make up a three component system - Or, Ab, and An are the shorthand designation of the three components. The way in which the two or three components can mix and form solid solutions with different proportions of each is complicated. It depends upon temperature, pressure, composition of the mixture, and the relative abundance of K, Na, Ca, Al, and other elements. The description of the solid solution is written with the shorthand designation of the components with a subscript denoting the percentage of the component. For example, Or<sub>26</sub>Ab<sub>66</sub>An<sub>8</sub>, is the designation of a feldspar (called anorthoclase) formed at high temperature.

One common solid solution series is plagioclase feldspar (Ca,Na)(Al,Si)AlSi<sub>2</sub>O<sub>8</sub>. Plagioclase feldspar is formed both at high and low temperatures but it contains only two components of the three component feldspar system, Ab and An. Na-rich plagioclase feldspar would have a designation such as Ab<sub>95</sub>An<sub>5</sub> and be composed of 95% NaAlSi<sub>3</sub>O<sub>8</sub> and 5% CaAl<sub>2</sub>Si<sub>2</sub>O<sub>8</sub>. Such a feldspar is called albite. Another example is Ab<sub>4</sub>An<sub>96</sub> - 4% NaAlSi<sub>3</sub>O<sub>8</sub> and 96% CaAl<sub>2</sub>Si<sub>2</sub>O<sub>8</sub>. Such a feldspar is called anorthite. Any other combination is also possible. Plagioclase feldspars made up of different solid solutions are given specific names which indicate

**Table 8.2.** Names of the divisions of the plagioclase series showing the abundance, range for the Ab end member component.

Plagioclase feldspar type	Ab end-member (%)
Albite	Ab <sub>100</sub> to Ab <sub>90</sub>
Oligoclase	Ab <sub>90</sub> to Ab <sub>70</sub>
Andesine	Ab <sub>70</sub> to Ab <sub>50</sub>
Labradorite	Ab <sub>50</sub> to Ab <sub>30</sub>
Bytownite	Ab <sub>30</sub> to Ab <sub>10</sub>
Anorthite	Ab <sub>10</sub> to Ab <sub>0</sub>

relative percentages of each component. Table 8.2 gives the names of the divisions of the plagioclase series showing the abundance range for the NaAlSi<sub>3</sub>O<sub>8</sub>, Ab end member component.

The pyroxene group is also an abundant group of minerals on Earth. The members of the group are closely related to one another, like the members of the feldspar group, and also crystallize in two different systems: orthorhombic and monoclinic. Again, the possibilities of different types and compositions are many and the cause of the differences are related to temperature, pressure, and abundance of elements present in the mix at the time of formation. Basically, there are Fe-rich, Mg-rich, Ca-rich, NaAl-rich, CaMn-rich, and "other"-rich pyroxenes. Examples of ortho-pyroxene are enstatite (MgSiO<sub>3</sub>) and hypersthene (Mg,Fe)SiO<sub>3</sub>. Examples of clinopyroxene are diopside (CaMgSi<sub>2</sub>O<sub>6</sub>), hedenbergite (CaFeSi<sub>2</sub>O<sub>6</sub>), and augite (intermediate between diopside and hedenbergite with some Al). There are others but this serves to give a general idea.

Another mineral series that is very common on Earth, especially in the mantle, is olivine (Mg,Fe)<sub>2</sub>SiO<sub>4</sub>. Like the feldspar system, it is a continuous solid solution of two end member components, Mg<sub>2</sub>SiO<sub>4</sub> and Fe<sub>2</sub>SiO<sub>4</sub>. They are called forsterite (Fo) and fayalite (Fa), respectively. The shorthand notation is similar to that for the plagioclase solid solution series. For example, an olivine composition might be Fo<sub>66</sub>Fa<sub>34</sub>.

Other minerals are sulfates, sulfides, carbonates, amphiboles, and micas, to name only a few. Earth has a rich diversity of thousands of minerals owing to its water-rich environment, plate tectonics, long volcanic history, and hydrologic cycle. Iron-titanium oxides are plentiful on the Moon but to date there is no evidence for their existence on Mercury. Mars has considerable water ice in its sub-surface material and at the polar regions. There is evidence for past flowing water and possible oceans on its surface, and surface weathering of its minerals, rocks, and soils. Mars soils are almost surely more diverse than the regoliths of the Moon and Mercury. They are certainly more altered by water processes than the regoliths of Mercury or the Moon. Mercury and the Moon, with no sign of plate tectonics or a hydrologic cycle, has an assemblage of rocks, minerals, and regoliths, probably limited to those that are associated with crystallization of *magma*, *extrusive* lava

flows, possible *igneous* intrusions, and meteoritic impact melting, fracturing, and mixing.

### 8.3 MERCURY'S SURFACE COMPOSITION

The past two decades of Mercury surface observations have resulted in many good observations that are continuously being refined and augmented. These observations include imaging in visible light (400–700 nm), near-IR (700–1000 nm) and mid-IR (2.5–13.5 nm) spectroscopy. Certain wavelength regions are blocked, or at least attenuated because of Earth's atmosphere. Terrestrial atmospheric  $\text{NO}_2$ ,  $\text{O}_3$ ,  $\text{CO}_2$ ,  $\text{CO}$ ,  $\text{H}_2\text{O}$ , and  $\text{CH}_4$  are the main absorbers between 400–1000 nm and 1.0–13.5 nm. Regions in the spectrum where light is attenuated by absorption from terrestrial molecules are called *telluric absorptions*. Some remove more of Mercury's light on its path through the atmosphere than others and in many cases proper corrections for the absorptions can be made to the spectra from Mercury so that they can be interpreted properly in terms of rock and mineral signatures. Sections of the Earth's atmosphere where no, or very little light can penetrate are called *opaque* to radiation and these spectral regions result in gaps in our knowledge about Mercury's spectrum. Regions of the spectrum where little or practically no attenuation of light by the Earth's atmosphere occurs are called *atmospheric windows*.

We have only a little knowledge of the chemical makeup of Mercury's surface. Thus, we shall limit our discussion to only the most common of rock types and rock forming minerals. A good candidate for a rock type on Mercury is low-iron basalt (see Chapter 10). The dominant rock type on the surfaces of Earth, Venus, and Mars is basalt. Basalt is a rock primarily composed of feldspar, pyroxene, and olivine. Another possible rock type on Mercury is anorthosite, a rock composed of more than 90% plagioclase feldspar with other component minerals like pyroxene. These are the two main rock types on the Moon. There is a wide range of possible compositions in both basalts and anorthosites.

Basalts and anorthosites have very different origins. Basalt is formed by a *petrogenetic* process called *partial melting*. As the temperature of a parent rock is increased the low-melting point fraction melts first and has a characteristic composition which rises and is erupted on the surface. This composition corresponds to the low-melting point composition of the parent rock. On the Moon both the mare and KREEP (potassium (K), rare earth elements, phosphorous (P)) basalts have characteristic low-melting point compositions that were produced by partial melting of a less differentiated rock in the interior of the Moon. Anorthosite, on the other hand, is formed by a process called *fractional crystallization*. In this process, when an igneous melt begins to cool and crystallize, the denser crystals sink through the residual liquid and the lighter (less dense) crystals float to the top. Therefore, layers accumulate in which one mineral is greatly concentrated. The lunar highlands anorthositic rocks are characterized by a super-abundance of one mineral, anorthite ( $\text{CaAl}_2\text{Si}_2\text{O}_8$ ). This composition is far removed from low-melting point liquids and was formed by fractional crystallization.

Recall from the discussions of albedo and slope, that Mercury's surface composition is different from that of the Moon even though they resemble one another morphologically. The compositional differences are likely to be rather subtle, however, like the relative amounts of Na, or K in the feldspar and the relative amounts of Mg, or Fe in the pyroxenes or their crystalline structure. But it is likely that Mercury has igneous rocks that either crystallized in place or flowed from fissures early in its history.

#### 8.3.1 Measuring surface composition with a telescope

Planetary astronomers use instrumentation on telescopes for compositional analyses of planetary surfaces. Light from the planet's surface carries information about the composition and structure of the dust, soils, rocks, and minerals in the regolith. The exact way in which light interacts with the regolith depends upon many factors. Some factors of major importance are: wavelength; temperature and thermal gradients; composition; and grain size. Measurements made in the laboratory of typical soils, rocks, minerals, meteorites, and lunar samples permit an understanding of what spectral features may be predicted for a given composition and grain size.

#### 8.3.2 Visible and near-IR spectroscopy

The power of visible and near-IR telescopic spectroscopy (400–2500 nm) has been demonstrated throughout the solar system for decades. For example, the size and shape of absorption bands in reflected light from the surface caused by crystal field transitions, metal-metal intervalence charge transfer transitions, and oxygen-metal charge transfer transitions of the materials in the regolith, are very diagnostic.

One of the best known features in reflectance spectroscopy of terrestrial bodies is an absorption caused by an electronic transition in an iron cation ( $\text{Fe}^{2+}$ ). The electronic transition occurs when Fe is bound to O in a lattice of a silicate. Planetary scientists familiar with this absorption band commonly refer to it as the FeO band. It occurs between 900 and 1000 nm in the reflected spectrum from a surface with FeO in the silicate portion of the regolith.

#### 8.3.3 The FeO band in lunar spectra

The origin of the Moon was poorly understood until the late 1980s. In attempting to put together a coherent hypothesis for the lunar origin, it was necessary to know the composition not only of the lunar surface but also of the deeper, more primitive materials of the lunar mantle. The lunar mantle is the region below the surface and crust on the Moon that exists undisturbed except by volcanism and deep, excavating impacts.

Prior to the *Apollo* missions that returned lunar surface samples for laboratory analysis, ground-based telescopic visible and near-IR spectroscopy was the best method for compositional studies. Several absorptions in the reflected light from

the lunar surface can be interpreted in terms of the cations in the minerals of the lunar regolith that absorb sunlight. These absorptions by  $\text{Fe}^{2+}$ ,  $\text{Mg}^{2+}$ , and other cations look different with small changes in the crystalline lattices that make up the rocks and rock debris. The best known of these absorption bands are probably the lunar olivine and pyroxene bands. Mapping the composition of the lunar near-side resulted in the identification of mantle material in Copernicus crater by measuring the depth, width, and the location of absorption minima in the bands. Comparisons with spectra of terrestrial laboratory samples aided in this accomplishment. The absorption features in the spectra shown in Figure 8.2 are examples.

### 8.3.4 The FeO band in Mercurian spectra

Only a dozen or so locations have been measured but from this evidence we deduce that Mercury's surface materials may contain at most, a few percent FeO in surface materials, and maybe in some locations, none at all. Some near-IR spectra are shown in Figure 8.3 along with some spectra of the Moon's surface for comparison. The

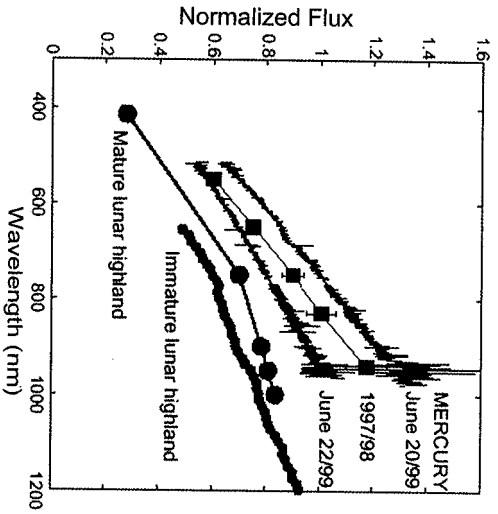


**Figure 8.3.** Comparison of the reflectance spectra of Mercury's surface with that of the Moon. The slopes of the spectra are similar from 400–800 nm, then the rate of increase of the lunar spectra drops. The Mercury spectra continue to rise at the same rate to 1000 nm. The depression beyond 800 nm in the lunar spectra is due to the presence of FeO in the lunar soil. The fact that there is no such dip in the Mercury spectra is evidence for low or no FeO in the Mercurian regolith at the locations measured and also for a more mature surface than the Moon (courtesy Johan Warell, Mercury spectra from the Nordic Optical Telescope and the Swedish Vacuum Solar Telescope).

feature in the spectrum that indicates the presence of FeO appears as a region of less steep rise in the lunar spectra. If there were measurable FeO in Mercury's soil the absorption would be at the same location on the x-axis, but no dip in the spectrum is seen. What is shown in the steeper slope of the spectrum indicating that Mercury's surface is very mature, more mature than the Moon's. It is very altered by space weathering mechanisms like meteorite bombardment, solar wind implantation, ion sputtering, photon sputtering, and cosmic ray impact and, to some extent, resembles the spectrum of Apollo 16 soil in Figure 8.2.

### 8.3.5 Mid-IR spectroscopy

Spectroscopic measurements of Mercury's surface at longer wavelengths (2.5–13.5  $\mu\text{m}$ ) have provided important chemical information about Mercury's surface. While absorption bands are created in the near-IR spectral region from electronic transitions in the molecules bonded in the lattices of silicates, in this mid-IR region, the absorption bands are caused by the vibration, bending, and flexing modes of the crystalline lattices. In the mid-IR spectral region it is possible to measure the thermal emission from the regolith. When rocks and soils are warm they emit light that has a spectral signature of their composition. This is also true of molecules in the atmosphere. By measuring the spectral features from the thermal emission from a planet's surface and atmosphere we can learn what materials are there. The location on the planet, for all data, is biased toward the hottest regions in the footprint of the *spectrograph aperture*.

Methods used to interpret mid-IR spectra include the following:

- (1) Identification of key spectral features diagnostic of composition. This has been achieved in the laboratory by measuring spectra from terrestrial and lunar surface materials like rocks, minerals, powders of rocks and minerals, and glassy volcanic material as well as glasses formed from rapid cooling of silicate melts.
- (2) Comparison of laboratory and telescopic mid-IR spectra of lunar soils from similar locations on the Moon.
- (3) Use of the same spectrograph to obtain spectra of rocks, minerals, and powders to compare to spectra of the Moon's and Mercury's surface and thus calibrate spectrograph performance and resulting spectral character.
- (4) Comparison of spectra, obtained from spacecraft above Earth's atmosphere, of objects in the Solar System (Jupiter, Saturn, asteroids) with those obtained from mid-IR instruments from ground-based observatories.

### 8.3.6 Volume scattering region

From 2.5 to 7  $\mu\text{m}$ , *volume scattering* of light from regoliths becomes important. There are absorption (and emittance) features associated with photons scattering in individual grains. Many silicates, sulfates, and carbonates have diagnostic features in this spectral region. Most of this spectral region is available to spectrographs at

high-altitude ground-based observatories and from stratospheric observatories like the Kuiper Airborne Observatory (KAO - retired) and the Stratospheric Observatory for Infrared Astronomy (SOFIA - to be commissioned in 2005).

Spectra from olivine and pyroxene, two minerals common in igneous rocks, exhibit emission peaks in the volume scattering region. Specifically, pairs of peaks near 5.7 and 6.0  $\mu\text{m}$  are diagnostic of olivine while a broad emission maximum near 5  $\mu\text{m}$  is diagnostic of pyroxene.

A strong 5  $\mu\text{m}$  emission feature in a Mercury spectrum from 45–85° longitude closely resembles that of laboratory clino-pyroxene powders. The best fit is to diopside ( $\text{CaMgSi}_2\text{O}_6$ ), and the low-FeO abundance indicated by near-IR reflectance spectroscopy supports a low-iron-bearing pyroxene. Spectroscopic observations of Mercury have been made in this spectral region from the KAO, and between 3 and 7  $\mu\text{m}$  from 13,786 ft altitude at Mauna Kea (the NASA Infrared Telescope Facility [IRTF]). Another emission feature, the emission maximum (EM), is also present in the spectrum. The wavelength of the EM is an important diagnostic of the weight percent of  $\text{SiO}_2$  in the silicate. This will be discussed in Section 8.3.7. Figure 8.4

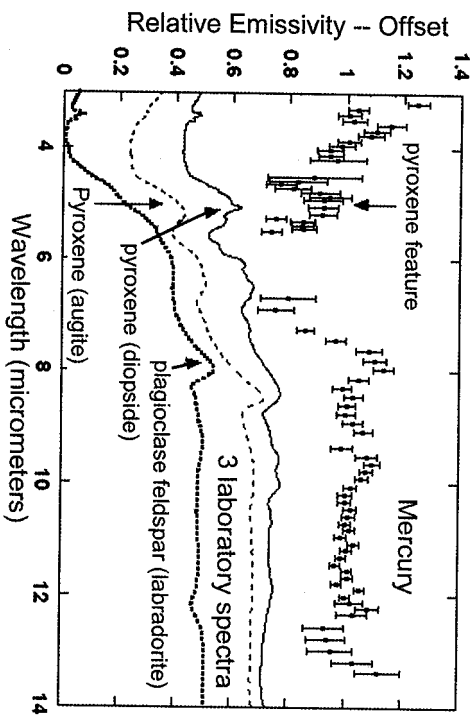


Figure 8.4. A spectral feature at 5  $\mu\text{m}$  in Mercury's spectrum from 45–85° longitude, resembles that exhibited in laboratory spectra from two samples of pyroxene. Also exhibited is an emissivity maximum (EM) at 7.9  $\mu\text{m}$  that is indicative of intermediate  $\text{SiO}_2$  content. Plagioclase feldspar of  $\sim 50\%$  also has an EM at this wavelength. Spectra such as these indicate that Mercury's surface, at these locations, has spectral characteristics similar to those of low-iron basalt, or anorthositic with plagioclase more Na-rich than lunar anorthositic (laboratory spectra from Salisbury *et al.*, 1986, 1991; Mercury spectrum from Sprague *et al.*, 2002).

shows the Mercury spectrum from 45–85° longitude along with some laboratory spectra of pyroxene and plagioclase feldspar for comparison. Unfortunately the two pieces of information (pyroxene and weight %  $\text{SiO}_2$ ) are not enough to uniquely identify the rocks that formed the regolith at this location. Powders of either low-iron basalt or anorthositic with about 90% plagioclase and 10% low-iron pyroxene could give the same features.

The recent reanalysis of *Mariner 10* imaging has also revealed new information about this region of Mercury's surface, especially around the region of Rudaki plains (3S, 56°W) and Tolstoj (16S, 164°W). Here smooth plains have *embayed boundaries* indicative of lava flow infills. Also scattering properties are similar to those of *pyroclastics* and glasses on the Moon. On the Moon, lava flows are basalt. On Mercury there is no evidence for the iron-bearing basalts so common on the Moon. However there is ample evidence for rocks formed from fluid lava flows. Such fluid lava flows could have the composition of low-iron basalts or other types of low viscosity lava (Figure 8.5).

### 8.3.7 Reststrahlen bands and emissivity maxima (EM)

Major rock-forming minerals have their fundamental molecular vibration bands in the region from 7.5 to 11  $\mu\text{m}$ . These features are called the Reststrahlen bands. The transparency feature between 11 and 13  $\mu\text{m}$  is associated with the change from surface to volume scattering. There are also major features in the region from 13 to 40  $\mu\text{m}$ , associated with the bending, twisting modes of silicates, and other solar system materials.

Emissivity maxima (EM) are associated with the *principal Christiansen frequency*, a silicate spectrum which usually occurs between 7 and 9  $\mu\text{m}$ . As mentioned above, EM are good diagnostics of bulk regolith or rock type (weight percentage  $\text{SiO}_2$ ), in powdery mixtures of rocks, minerals, and glasses common in regoliths. The EM is also a spectral diagnostic of specific mineral identity.

On Mercury, EM at or close to 7.9–8.0  $\mu\text{m}$  occur in spectra from 12–32°, 22–44°, 40–45°, 45–85°, 10–75°, and 110–120° longitude (Figure 8.6 and 8.7), indicative of intermediate silica content ( $\sim 50$ –57%  $\text{SiO}_2$ ). These locations are in the intercrater plains east of the crater Homer.

Based on the spectrum shown in Figure 8.7 and from other spectra of Mercury's surface, it may be that Mercury's regolith has a high concentration of plagioclase feldspar, perhaps labradorite  $\text{NaAlSi}_3\text{O}_8$   $\text{CaAl}_2\text{Si}_2\text{O}_7$ . An alternative explanation for the apparent match to plagioclase feldspar is that the spectrum comes from the glassy soil on Mercury's surface that is very mature after long periods of meteoritic bombardment. Scientists have shown that if lunar soils are very mature, much of the  $\text{FeO}$  is removed from the glasses and they appear much more feldspathic (like feldspar) in laboratory spectral measurements.

Many smaller dips in the Mercury spectrum are not present in the spectrum from the laboratory sample. These features may be in the Mercury spectrum because Mercury's surface is much hotter than the environment of the chamber holding the laboratory sample. Alternatively, the features may be from other minerals that

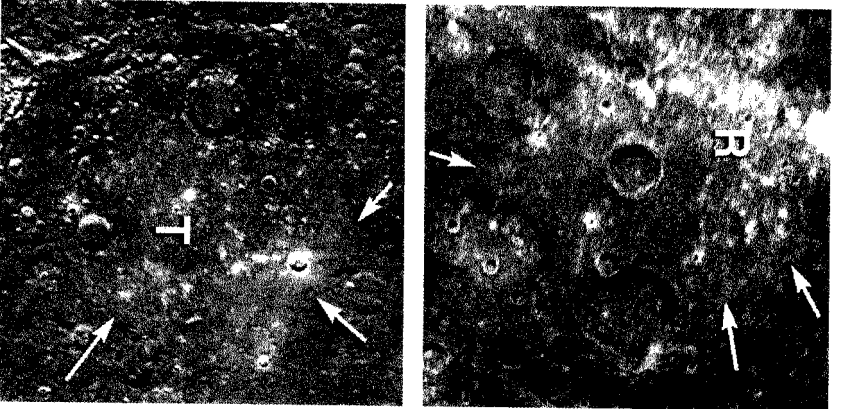


**Figure 8.5.** Spectra from equatorial regions at 45–85° longitude shown in Figure 8.4, come from the region on Mercury's surface shown in the top image. Rudaki (R) is a region where multi-spectral analysis has revealed evidence for volcanic flow fronts and pyroclastics. In the lower image of Tolstoj (T) regions of embayments from apparent lava flows are also indicated with arrows. (adapted from Robinson and Taylor, 2001).

were not in the model. It is also possible that some of the smaller features are noise in the Mercury spectrum and do not represent spectral features from materials on Mercury's surface. Spectra from 68–108° and 100–160° longitude have multiple EM indicating a more complicated bulk composition and/or mixed mineralogy of lower SiO<sub>2</sub> content (more mafic) basic composition, 45–49% SiO<sub>2</sub>).

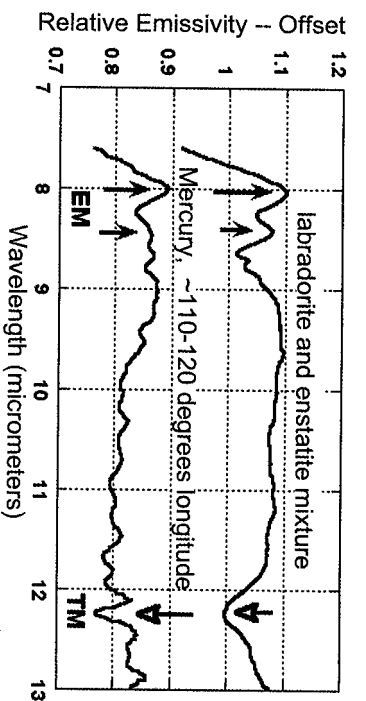


**Figure 8.6.** Shows an example of one of these Mercury spectra compared to a laboratory spectrum from a mixture of plagioclase feldspar and the Mg-rich ortho-pyroxene called enstatite. The EM and the transparency minima (TM) are marked with arrows. Spectra obtained in the laboratory from powdered samples of silicates and aluminosilicates are often found to be similar to spectra from Mercury. The wavelength and the shape of the EM at 8.0  $\mu\text{m}$  is the same for the Mercury spectrum and the model spectrum. The wavelength of the TM for Mercury the model also matches. Differences between the two spectra in the Reststrahlen bands can also be seen but are not yet explained. Adapted from Sprague and Roush (1998).

### 8.3.8 Transparency minima (TM)

The TM between 11 and 13  $\mu\text{m}$  is associated with the change from surface to volume scattering. Generally the wavelength where the minimum occurs is a good indicator of the weight percent SiO<sub>2</sub> present in a rock powder. Because of historical geologic circumstance, the divisions of SiO<sub>2</sub> are designated by the terms acidic, intermediate, basic, and ultrabasic. The range of wavelengths for transmission minima and the weight percent SiO<sub>2</sub> content for some common rock powders are shown in Table 8.3.

The classification of silicates according to weight % SiO<sub>2</sub> has been replaced in some cases by classification according to mineralogy. For the discussion in this chapter we prefer the older nomenclature but include the newer parenthetically in Table 8.3 and point out that the SiO<sub>2</sub> values are appropriate for typical samples.

The Mercury spectrum from 110–120° longitude in Figure 8.6, has a clear and strong transparency minimum at 12.3  $\mu\text{m}$  that is at the same location as the transparency minimum in a laboratory spectrum of labradorite powders or some low-iron basalt. This is consistent with the location of the EM in the same spectrum as described above. Spectra from longitudes centered on 80°, 256°, and 266° have probable transparency minima at 12  $\mu\text{m}$ . The bulk composition associated with a transparency feature at this wavelength is intermediate to basic (45–57 weight % SiO<sub>2</sub>). Spectra from a region centered on 15° has a minimum at 12.5  $\mu\text{m}$  indicative of about 44 weight % SiO<sub>2</sub> or an ultra-basic composition. A spectrum from a region



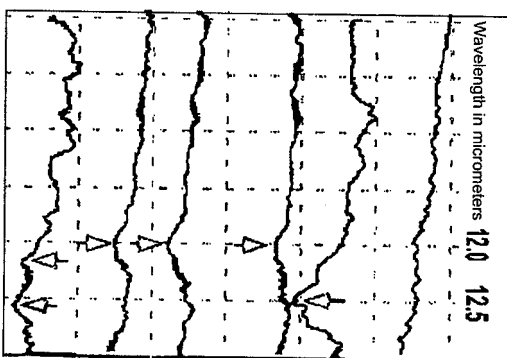


Figure 8.7. Spectra from Mercury's surface at 6 different locations, show TM from top down at longitudes centered on: 10°, 15°, 256°, 266°, 80°, and 229° respectively. Wavelengths are between 12 and 12.7  $\mu\text{m}$ . Such spectral features are indicative of the weight %  $\text{SiO}_2$  in the soil at the location measured. Generally, the shorter the wavelength of the TM, the more  $\text{SiO}_2$  in the silicate (see text for more details) (adapted from Cooper *et al.*, 2002).

Table 8.3. Wavelength ranges for TM and weight percentage  $\text{SiO}_2$  for common rock powders.

Designation	Weight % $\text{SiO}_2$	Rock powder (intrusive)	Rock powder (extrusive)	Wavelength ( $\mu\text{m}$ ) of TM
Acidic (felsic)	62-75	Granite	Rhyolite	11.5-11.7
Intermediate	52-61	Diorite	Andesite	11.8-12.1
Basic (mafic)	46-51	Gabbro	Basalt	12.1-12.4
Ultrabasic (ultramafic)	39-45	Peridotite	Picrite	12.4-12.7

centered on 229° longitude has a doublet transparency minimum. Figure 8.7 illustrates these spectral features with 6 spectra from Mercury's surface obtained with the McMath Pierce Solar Telescope near Tucson, Arizona.

About 40% of Mercury's surface has been measured spectroscopically. Roughly speaking the coverage is of the equatorial and low latitude regions at most, but not all, longitudes. From these observations we know that Mercury's surface composition is heterogeneous. Regions near Homer and the Murasaki crater complex appear feldspathic, trending toward  $\text{Ab}_{70}\text{-Ab}_{40}$ , more Na-rich than the lunar anorthosites.

Bulk compositions are of intermediate silica content. Some mixed compositions of lower silica content are present in the regions from 68–160° longitude, but not at all locations measured. One candidate for the rocks at these locations is low-iron basalt – mixtures of feldspar, pyroxene, and minor olivine of intermediate (52–57 weight percent) or basic (46–51 weight percent)  $\text{SiO}_2$ .

Regions west of Caloris appear to have mixed mineralogy and a more complex bulk composition with some basic and ultrabasic regolith types. According to transparency minima, an ultrabasic composition falls east of the Homer crater near 15°. Two measurements indicate that ultrabasic regolith types are located far west of Caloris from about 205° longitude. Feldspathoids, alkali-rich aluminosilicates with low (39–45 weight percent)  $\text{SiO}_2$ , such as tephrite or basanite are possible extrusive rocks that could be in this region. Such rocks are formed from plagioclase bearing lavas in which feldspathoids are present in greater abundance than 10 weight percent. Tephrites have little olivine while basanites may have considerable olivine. There is evidence for ultrabasic-like soils at 205–240° longitude. Peridotite and dunite are olivine-rich low  $\text{SiO}_2$  rocks. It would not be surprising to have low-iron olivine in these regions but no signature identified as olivine has yet been found.

This interpretation is very generalized because the areal extent of the spatial footprint is no smaller than 200 km by 200 km for the very best spatially resolved observations, and as much as 1000 km by 1000 km for the least spatially resolved region. On the surface of Mercury viewed by *Messenger* these large areas mostly encompass a variety of morphologically different terrains that could have different compositions.

### 8.3.9 Comparison to the Moon

Hundreds of kg of lunar samples were brought back by *Apollo* astronauts. Some of those samples have been measured in the laboratory with spectrometers to examine and compare their spectral signatures from location to location.

A spectrum from equatorial regions near 20–25° longitude on Mercury's surface is shown and compared to laboratory spectra from a *particulate breccia* sample brought back from the *Apollo 16* landing site on the Moon (Figure 8.8). The lunar sample is ~90% anorthite (Ca-feldspar) and ~10% pyroxene. The EM for both spectra is centered close to 8  $\mu\text{m}$  and marked with an arrow. The wavelength of the EM indicates a *feldspathic* rock type. Other features in the Mercury spectrum are also similar to the lunar spectrum and indicate the presence of pyroxene on Mercury's surface.

Based on these observations and others in the near-IR region of the spectrum, some scientists who specialize in the petrology of the lunar surface think that lunar anorthosites provide the best analogue for the composition of Mercury. Also there are examples of meteorites with little or no oxidized iron such as the *enstatite chondrites* and *achondrites*. These meteorites formed in a *reducing* environment and have sulfides present. It has been suggested that Mercury may have formed in a similar environment. One argument against this theory is that mid-infrared spectra

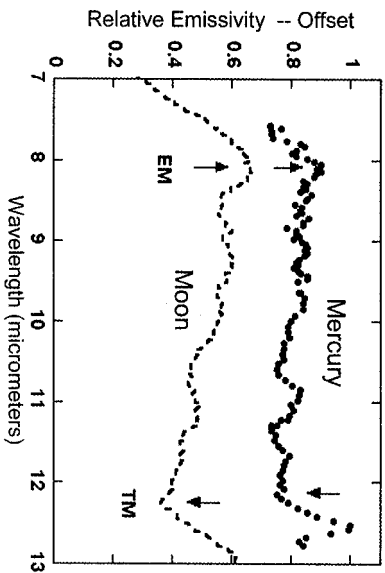


Figure 8.8. A spectrum from Mercury's equatorial regions at about 20–25° longitude is shown along with a laboratory spectrum of a sample from the Moon. The lunar sample is a particulate breccia #67031 (composed of feldspar and pyroxene) from the *Apollo 16* landing site (mercury spectrum from Sprague *et al.*, 1996; lunar spectrum from Nash and Salisbury, 1991).

from Mercury's surface do not resemble laboratory mid-infrared spectra from such meteorites. Of course as more data become available, this position may change.

#### 8.4 WHERE IS THE IRON AT MERCURY?

Mercury has a large, high density core which is probably composed of mostly iron with the addition of some lighter elements such as sulfur. Issues regarding Mercury's core were partially discussed in Chapter 5 and will be discussed in more detail in Chapter 12. As discussed above, there is little evidence for FeO on Mercury's surface in any data set. This is certainly one of the most interesting puzzles about Mercury. Has all of Mercury's iron gone into the core and left none behind in the regolith, crustal rocks, or mantle?

##### 8.4.1 Other terrestrial planets and the asteroid belt abound with oxidized iron

Venus, Earth, the Moon, Mars, and many asteroids have several percent oxidized iron in their surface rocks and minerals. The abundance of oxidized iron (FeO or Fe<sub>2</sub>O<sub>3</sub>) for example, has been measured or inferred in a variety of ways – no one way is suitable for every rocky body. For Venus, the *Venera 13* and *14* landers made *in situ* fluorescent X-ray emission measurements of the soil and cores from a drilling experiment. At the *Venera 13* site a high potassium basalt was discovered that is similar to mid-oceanic ridge basalts. At the *Venera 14* site the rock composition is

Table 8.4. Abundance of FeO in surface rocks and regolith inferred from measurements of terrestrial planets, the Moon, and some asteroids.

Terrestrial Body	Typical weight % FeO
Mercury	1–3
Venus	8–10
Earth	5–28
Moon	4–27
Mars	10–40
Asteroids	4–25

similar to plateau basalts on Earth. These basalts have an FeO content of from 8–10 weight percent. The Earth's surface basalts have an FeO content ranging from <2 to 28 weight percent. For the Moon, remote sensing from Earth-based telescopes and returned lunar samples from the *Apollo* and *Luna* missions show 4–27 weight percent FeO. Meteorites from Mars, and remote sensing from Earth-based telescopes and orbiters indicate a FeO content of 10–40 weight percent. For asteroids, near-IR spectroscopy has revealed a wide variability in iron content ranging from 4 to 25 weight percent. But almost all asteroids in the asteroid belt show some hint of the famous reflectance absorption features that indicate oxidized iron in pyroxene or olivine, or both. A comparison of the abundance of FeO in surface rocks and regolith inferred from many measurements of all the terrestrial planets, the Moon, and some asteroids is given in Table 8.4. Iron content in meteorites ranges from almost all to practically none.

##### 8.4.2 For Mercury, low oxidized iron

All the telescopic spectral evidence (near-IR, mid-IR, and radio wavelengths) for Mercury suggests that its surface is low in oxidized iron. This suggests that Mercury is a chemically unique terrestrial planet. This also places severe constraints on Mercury's origin as discussed in Chapter 12. These measurements indicate that the FeO content is from 1–3 % at most. As mentioned above, it could be that space weathering has converted most of the FeO to iron metal but this explanation fails to meet the constraints of the radio centimeter wavelength observations that show Mercury's regolith to be more transparent (lower in iron and iron metal and titanium) than the Moon.

Recalibrated *Martiner 10* images taken in the UV (375 nm) and orange (575 nm) wavelengths indicate compositional variations in the Mercurian surface consistent with those deduced by earth-based spectroscopic observations. These newly calibrated color images have been interpreted according to the view that ferrous iron lowers the albedo and reddens a lunar or Mercurian soil. These data suggest that the average hemispheric FeO content is less than 3% by weight, which is consistent with Earth-based measurements. Furthermore, the color images show color boundaries

between smooth plains and the surrounding terrain indicating compositional differences. In at least two cases the smooth plains overlie material that is bluer (higher UV/orange ratio) and is enriched in opaque minerals relative to the hemispheric average. Since the smooth plains are probably old lava flows (see Chapter 10), and the FeO solid/liquid *distribution coefficient* is about 1% during partial melting, it is estimated that the Mercury's mantle has a FeO abundance similar to the lava flows (less than 3%). But this is very sensitive to the degree of partial melting.

## 8.5 SUMMARY

Both Earth-based spectroscopic observations and calibrated *Mariner 10* images indicate that the surface of Mercury is heterogeneous in composition with a wide range of SiO<sub>2</sub> content. The FeO content appears to be between 1 and 3% which is abnormally low compared to other terrestrial planets and the Moon. Evidence for pyroxene appears to be of the Mg-rich or Ca-rich type. The spectroscopic data are consistent with compositions ranging from low-iron basalts and anorthosites. There are also spectra that exhibit similarities to laboratory spectra of *spinelite*. However, to have a rock so highly evolved petrologically requires multiple episodes of partial melting which may be problematical for Mercury.

Photometry of Mercury's surface in the UV and visible indicates Mercury is fairly smooth, consistent with flooding by lavas. The morphology of the land forms, which will be discussed in detail later in Chapter 10, indicate fluid lava flows over much of the surface. *Mariner 10* imaging ratios indicate bright excavated regions. Ground-based spectroscopy indicates that these excavated regions may be anorthosites. This would be consistent with the appearance of enhanced regions of Na atmosphere that are associated with the fresh craters as discussed in Chapter 6. Continued ground-based observations and detailed measurements by *MESSENGER* should greatly expand our knowledge of the variety of compositions and their spatial distribution.

# 9

## The impact cratering record

### 9.1 MERCURY'S MOST COMMON LANDFORM

Mercury is one of the most heavily cratered planets in the Solar System, and its cratering record provides important information on the cratering process and crater characteristics in that part of the Solar System. Because Mercury is the innermost planet, it provides important constraints on the origin of impacting objects in the terrestrial planet domain.

#### 9.1.1 It all began with the Moon

In 1609 Galileo recognized and wrote about craters he viewed with the recently invented telescope. The craters he saw, were common on the Moon. In fact, the most common landforms in the Solar System are impact craters. They occur in greater or lesser abundance on almost all solid bodies explored to date.

#### 9.1.2 Three basic crater characteristics

There are three basic characteristics common to all relatively fresh impact craters:

- (1) a near-circular raised rim;
- (2) a floor that is deeper than the crater surroundings; and
- (3) a relatively rough *ejecta blanket* that surrounds the crater.

Small craters have bowl-shaped interiors and are called simple craters. Larger craters have terraced inner walls, a relatively flat floor, *central peaks* and are called complex craters. The rim structure consists of a flap of overturned material resulting in inverted *stratigraphy* (older on top and younger on the bottom). The crater is surrounded by an extensive ejecta deposit consisting of two parts: a relatively narrow inner zone of continuous hummocky ejecta; and an outer zone consisting